

Modelling of undercutting and failure of non-cohesive riverbanks

M. H. Nasermoaddeli & E. Pasche

Institute of River and Coastal Engineering, Technical University of Hamburg, Germany

ABSTRACT: Modelling of riverbank erosion has been a major interest among the researchers in the last few decades, but still little progress has been attained in bank evolution modelling in non-cohesive soils. This is mainly due to the incomplete understanding of the dominant processes and too simplified theoretical concepts used to describe the processes. The recent investigations of the authors on bank erosion process showed that undercutting of the riverbank, avalanche of the submerged zone of the bank, as well as failure of the overhang are the dominant processes in non-cohesive (sandy) riverbank erosion. A novel approach has been developed to model these processes by introducing a conjugated domain concept, in which hydrodynamic, sediment transport and bed evolution equations are described on finite element computational domain, while bank evolution is computed and simulated on a morphological domain. The bank evolution model includes avalanche and cantilever failure (tensile and shear types) processes. Pore pressure distribution in the riverbank has been approximated using an analytical function. The new developed numerical model was verified by field measurements. The simulation results showed that the proposed model has enhanced the simulation accuracy up to six fold in comparison to the earlier methods.

Keywords: River bank erosion, Modeling, undercutting, Cantilever failure, Non-cohesive

1 INTRODUCTION

In the process of lateral migration of the river channel, bank erosion plays the most important role. Study of the riverbank erosion is a key issue in meander restoration programs, which are often essential for rehabilitation of aquatic life. Land loss due to the riverbank retreat have a strong impact on floodplain dwellers, agricultural lands on the margins of the rivers, bridge crossings, bank protection works and other hydraulic constructions. Neglecting this process during flood events may result in underestimation in risk analysis of flood prone areas.

Therefore, it is not surprising that several research works have been achieved, especially in last two decades, to model bank erosion process (for example Mosselmann,1992; Kovacs and Parker, 1994; Shimizu *et al.*, 1996; Nagata *et al.*, 2000; Schmautz,2003; Chen and Duan,2006; Darby *et al.*,2007; Rinaldi, et al,2008). A review of several other research works can be found in ASCE Task Committee (1998a, 1998b).

Apart from different numerical and mathematical approaches applied in the mentioned works, what distinguishes them substantially, is the number of physical processes considered in their approaches. However, the reliability of numerical models do not exclusively lie on the number of processes being modelled, but (as well as) on the fact that to what extent the applied mathematical approaches are capable to describe the physical process being modelled. The latter depends on how well these processes have been understood. Hence, a plenty of researches have been devoted to improve the knowledge on bank erosion process and mechanisms in the last two decades, especially recently, which are summarized in the following.

1.1 Riverbank erosion process

It is well-known that riverbank retreat occurs both by continuous fluvial erosion as well as abrupt bank failure (Thorne,1982; Lawler *et al.* 1997;ASCE Task Committee, 1998;etc.). Riverbank-toe erosion causes to increase the bank

height and the slope of the bank to the extent that eventually riverbank mass failure occurs (Carson and Kirkby, 1972; Thorne, 1982; Simon *et al.* 2000).

Abrupt bank failure in cohesive soils is in form of rotational (circular) or planar failure surfaces (Thorne, 1982). While in non-cohesive soils, bank failure is mainly due to dislodgement and avalanche of the individual particles in submerged area of the bank with higher slope than the angle of repose, or due to shear failure along shallow, very slightly curved slip surfaces (ASCE Task Committee, 1998). Consolidation and cementation increases the stability of natural non-cohesive slopes beyond its critical angle of repose, specially in fine sandy soils.

Eroding of underlying non-cohesive layers creates overhang in cohesive soils which may eventually fail in either of three modes: shear, beam and tensile failure (Thorne and Tovey, 1981). Shear and beam failure result in a similar vertical bank profile after failure. Beam failure is a result of tension cracks in the overhang. Tensile failure occurs when only the lower part of an overhang block fails along an almost horizontal failure surface.

In the last decade an appreciable advancement has been attained in understanding the mechanism and processes involved in bank failure. Positive pore water pressure in the riverbank acts to reduce bank stability, particularly in rapid draw down stage in channels following a high flow (ASCE Task Committee, 1998, Simon *et al.* 2000, etc.). The negative pore water pressure above the water surface acts as an apparent cohesion and resists against failure, which increases the overall stability of the bank in cohesive soils (Casagli, *et al.*, 1997, 1999; Curini, 1998; Simon *et al.*, 2003, Rinaldi, *et al.*, 2004) as well as local stability of the unsaturated zone in non-cohesive (sandy) soils (Nasermoaddeli and Pasche 2008). Confining pressure of the water stage in the river increases the stability of the cohesive riverbank (Darby and Thorne, 1996; Casagli, *et al.* 1999), which may not hold for the non-cohesive soils (Nasermoaddeli and Pasche 2008).

Seepage out of the riverbank removes finer sediments and results in local failure of the bank referred to sapping (Ullrich *et al.*, 1986; Hagerty, 1991; Fox *et al.*, 2007; Wilson *et al.*, 2007 and Cancienne *et al.*, 2008), which results in formation of cavities or undercutting zones in the riverbank. This process is one of the important destabilizing factors, especially in non-cohesive (sandy) soils.

Undercutting process in sandy riverbanks, due to the bank-toe erosion and cantilever failure, has been studied with respect to the dynamics of the flow by Nasermoaddeli and Pasche (2008). When

the flow is not bank full in such rivers, the failure surface comprises primarily and mainly the submerged part of the bank. This is in sharp contrast to the failure mechanism in cohesive soils, in which the failure block extends via tension cracks up to the top of the bank (Osman and Thorne, 1988; Darby *et al.*, 2000).

Bank-toe is eroded due to the fluvial erosion resulting in local steepening of the riverbank in the submerged area (Fig. 1-A). It can be postulated that as soon as the submerged riverbank local slope reaches beyond its consolidated angle of repose (ϕ^c), the bank material of the over-steepened area (up to the water surface) slides in a shallow layer (in a cascade form) into the scoured bank-toe leaving a hanging zone over the water surface and an undercutting zone under the water surface (Fig. 1-B). This process introduces a complex bank geometry comprising vertical as well as negative slope in the undercutting and overhang zones.

Matric suction (negative pore water pressure) together with consolidation in the unsaturated zone of the bank act as an (apparent) cohesion force to stick the fine sand particles together enabling the formation of the overhang. The overhang can be further stabilized due to cementation and the small vegetation roots.

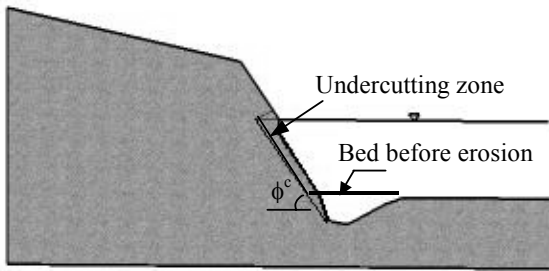
The failed bank material deposits at bank-toe in form of a slump or with saturated angle of repose (ϕ^s) as shown in Fig. (1-B), or transported as bed and wash load depending on the local flow and sediment transport capacity and sediment size.

Therefore, three different zones can be distinguished on the incised riverbank according to their slopes (Fig. 1-b), which are induced due to different geotechnical and fluvial processes. This distinguishes mainly from earlier works, in which generally one angle of repose has been considered as the stability criterion of the whole bank slope in non-cohesive soils and a parallel bank retreat has been assumed (Hasegawa, 1981; Nagata *et al.*, 2000; Jang and Shimizu, 2005; Duan *et al.*, 2001; Hafner, 2008). Furthermore, in earlier works, formation and stability analysis of the overhang in non-cohesive riverbank has not been considered.

In the following, a mathematical model to simulate bank erosion process in non-cohesive sandy soils is presented. Undercutting due to bank-toe erosion, cantilever failure (shear and tensile types) and the effect of vegetation (Cancienne *et al.*, 2008) are considered in this model. Since non-cohesive bank failure in saturated portion is not deep-seated in the bank, as in cohesive soils, the effect of the sharp gradient of phreatic line in the vicinity of the bank surface (or failure plane)

has been neglected, assuming to be in equilibrium with water stage in the river. This issue should be further studied by application of the seepage models.

A)



B)

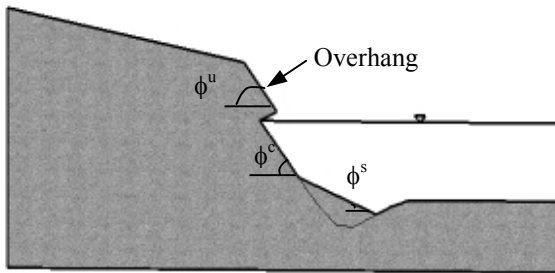


Figure 1. Schematic demonstration of undercutting process in non-cohesive banks. A) prior to the bank slide. B) After bank slide.

The mathematical model has been integrated into the morphodynamic model of RMA10s-Kaylps and verified by field measurement. The result of field measurements has been already presented in Nasermoaddeli and Pasche(2008).

2 MATHEMATICAL APPROACH

The generally accepted practice to model morphological evolution is the integration of hydrodynamic and sediment transport with a morphological model (bed and bank evolution models). In the following the hydrodynamic model is presented followed by sediment transport and morphodynamic model.

2.1 Hydrodynamic model

The governing equations of shallow flow in rivers can be described by the 2D depth-averaged Navier-Stokes' equations as follows:

$$\frac{\partial h}{\partial t} + u \frac{\partial h}{\partial x} + v \frac{\partial h}{\partial y} = 0 \quad (1)$$

$$\frac{\partial u}{\partial t} + u \frac{\partial u}{\partial x} + v \frac{\partial u}{\partial y} = -g \frac{\partial}{\partial x} (z_0 + h) + \frac{1}{\rho h} \frac{\partial (h \tau_{xx})}{\partial x} + \frac{1}{\rho h} \frac{\partial (h \tau_{xy})}{\partial y} + \frac{\tau_{w,x} - \tau_{b,x}}{\rho h} \quad (2)$$

$$\frac{\partial v}{\partial t} + u \frac{\partial v}{\partial x} + v \frac{\partial v}{\partial y} = -g \frac{\partial}{\partial y} (z_0 + h) + \frac{1}{\rho h} \frac{\partial (h \tau_{xy})}{\partial x} + \frac{1}{\rho h} \frac{\partial (h \tau_{yy})}{\partial y} + \frac{\tau_{w,y} - \tau_{b,y}}{\rho h} \quad (3)$$

where h = water depth, t = time, ρ = water density, g = gravity, z_0 = bed elevation, u and v = depth-averaged velocities in x and y directions, respectively. τ = depth-averaged Reynolds shear stresses (indices show the tensor direction). τ_w and τ_b = wind and bed shear stresses, respectively. Eq. (1) is the 2D depth-averaged continuity equation and Eqs. (2) and (3) are 2D depth-averaged momentum equations in x and y directions, respectively. Coriolis Force and dispersion terms are not included in the above equations. Applying eddy-viscosity concept of Boussinesq, the Reynolds shear stresses can be described as follows (in tensor form) :

$$\tau_{ij} = -\overline{u_i' u_j'} = \nu_t \left(\frac{\partial u_i}{\partial x_j} + \frac{\partial u_j}{\partial x_i} \right) - \frac{2}{3} k \delta_{ij} \quad (4)$$

where τ_{ij} = Reynolds stress tensor in ij direction with $i,j=1,2$ ($1=x$ and $2=y$ directions), u_i' and u_j' = instantaneous velocity fluctuation components with bar over them indicating time-averaged values, ν_t = eddy viscosity, u_i and u_j = depth-averaged velocity components, δ = Kronecker delta, and k = turbulent kinetic energy which is defined as follows:

$$k = \frac{1}{2} (\overline{u'^2} + \overline{v'^2} + \overline{w'^2}) \quad (5)$$

A turbulence model is required to model the eddy viscosity and close the above shallow water equations (Eq. 1-3). Among different available turbulent models (zero equation to two equation and Reynolds stress models, Rodi, 1993), Smagorinsky turbulent model has been applied here, which reads as follows:

$$\nu_t = (c_s \Delta)^2 \left[2 \left(\frac{\partial u}{\partial x} \right)^2 + 2 \left(\frac{\partial v}{\partial y} \right)^2 + \left(\frac{\partial u}{\partial y} + \frac{\partial v}{\partial x} \right)^2 \right]^{\frac{1}{2}} \quad (6)$$

where c_s = empirical factor between 0.065 to 0.23 (Forkel, 1995) and Δ = (area of the grid)^{1/2}.

2.2 Sediment transport

It is assumed that sediment transport is in equilibrium condition, implying that if the sediment concentration is greater than sediment transport capacity, net deposition takes place, whereas if sediment concentration is less than transport capacity net bed erosion occurs. The total sediment transport can be computed using depth-averaged advection-diffusion equation as follows:

$$h \left(\frac{\partial c}{\partial t} + u \frac{\partial c}{\partial x} + v \frac{\partial c}{\partial y} \right) - \frac{\partial}{\partial x} \left(\Gamma_x h \frac{\partial c}{\partial x} \right) - \frac{\partial}{\partial y} \left(\Gamma_y h \frac{\partial c}{\partial y} \right) - S_{bank} - S = 0 \quad (7)$$

where c = total depth-averaged sediment concentration, $\Gamma = \nu_t / \sigma$ turbulent diffusion coefficient (σ = Schmit number), S_{bank} = rate of bank erosion, S = net rate of sediment deposition(-) or erosion(+), which is computed as follows:

$$S = \frac{h}{t_c} (c_{eq} - c) \quad (8)$$

where c_{eq} = equilibrium total sediment concentration and t_c = an adaptation time scale for deposition or re-suspension of sediment.

To compute equilibrium total sediment transport (c_{eq}), the equilibrium bed load and suspended load concentration has been computed separately using the method of van Rijn (1984a,b) and summed up together.

It is recognized by the authors that modeling suspended and bed load transport separately (either as equilibrium or non-equilibrium formulation) may improve the sediment transport modeling, however, the focus of this work has been primarily on modeling bank retreat process.

2.3 Bed evolution

To model bed elevation change due to the net erosion or deposition the following equation was applied (King,2005):

$$\rho_s (1 - \lambda) \frac{\partial z_0}{\partial t} = \frac{h}{t_c} (c - c_{eq}) \quad (9)$$

where λ = bed porosity, ρ_s = bed sediment density and the rest of the parameters have been already declared. In the literature, other forms of the above equation can be found (for example, Phillips and Sutherland, 1989).

2.4 Bank evolution

The above-mentioned new concept of three angle of repose (bank-toe, undercutting zone and overhang zone) has been applied to model bank-erosion process in the present work.

Based on the field measurements (Nasermoadeli and Pasche,2008) the slope of failure plain in case of cantilever failure (shear failure) may vary from a steep positive to a negative value. However, only steep positive values are considered here. The failure of the overhang occurs when the safety factor (Eq.10) is less than 1.

$$SF = \frac{(c_r L_{eff.} + \psi \tan \phi^b - W \cos \phi^u \tan \phi^u)}{(W \sin \phi^u)} \quad (10)$$

where SF= safety factor; c_r = cohesion due to the root reinforcement; $L_{eff.}$ = the effective length (area per width) of the root zone. ψ is force produced by matric suction on the unsaturated part of the failure surface (kN/m); W =weight of the soil block (kN); ϕ^u =most critical slope of the failure surface of the unsaturated consolidated soil of the overhang, which should be determined as a calibrating parameter or on-site measurements, and ϕ^b = friction angle. The term ϕ^b varies for all soils, and for a given moisture content (Fredlund and Rahardjo, 1993), having a normal range of 10-20° (Simon *et al.*, 2000, Casagli *et al* 1999). Data on ϕ^b are particularly lacking for alluvial materials, which should be calculated by measurements using Tensiometer or similar devices.

Pore pressure distribution in the riverbank can be modelled using Richards equation (Dapporto *et al.*,2001,2003; Rinaldi *et al.*,2004 and Darby *et al.*, 2007,Rinaldi *et al.*, 2008). However, as already mentioned, due to assumption of equilibrium state with water stage in the river this approach was not followed. As a simplification, the pore water pressure was approximated by a simple quadratic function (similarly a linear function has been applied by Langedoen and Simon, 2008). In the submerged zone of the bank, pore pressure has been considered to be hydrostatic.

Furthermore, it is assumed that if the overhang is submerged due to the water rise in the river, the submerged portion would collapse in form of tensile failure (Thorne and Tovey,1981) immediately due to loss of matric suction (equilibrium state with water stage in the river). This assumption may lead to significant difference with the actual pore pressure in submerged zone of the overhang, depending on the duration of submergence. To the extent of the knowledge of the authors, there is still no study available on the pore pressure distribution in partly submerged overhang blocks. This will be a part of the future work of the authors team.

Two methods for distribution of eroded bank materials have been applied. In the first method, the whole eroded material due to the all three possible modes of erosion (avalanche, tensile and cantilever failure) are summed to a lump mass and distributed using a cumulative mass distribution function over bank-toe. Alternatively, the eroded materials resulting of each mode of erosion are passed separately to Eq.(7) as a source term.

3 NUMERICAL APPROACH

The above-mentioned riverbank erosion model has been integrated into the RMA10s-Kalypso model, which is based on the well known finite element fluvial model of RMA10s (King,2005).

At each time step, hydrodynamic and sediment transport models are solved decoupled. After updating bed elevation based on the Eq.(9), the stability of the submerged zone of the river is examined, with the method already described. It is then controlled for a probable tensile failure of the submerged part of the overhang. Finally, the stability of the overhang is examined using Eq. (10). The finite element nodes are updated after distribution of eroded materials using the either methods described above. At each time step the above procedure is repeated.

Formation of undercutting and overhang result in vertical and negative slopes in the bank topography, which is not allowed in numerical mesh of 2D depth-averaged models. Even in 3D hydrodynamic models, which apply layered 3D elements, such deformations are not permissible. To solve this problem, a morphodynamic domain conjugate to the finite element mesh was defined, on which the complex river bank evolution is modeled.

Hydrodynamic, sediment transport and bed evolution models are solved on the finite element domain. Each finite element node along the cross sections, under bank erosion study, is linked with a profile node in morphodynamic domain. The nodes in both domains are allowed to be vertically displaced, while the profile nodes at the front of the undercutting at the lower(inner) edge of the overhang as well as the outer edge of the overhang are allowed to be adapted laterally and vertically. The former is the case by developing undercutting (state 1 in Fig.2) and the latter by occurrence of tensile failure (state 2 in Fig.2).

As it is observed form this figure, all of the FE-nodes in submerged zones belong to the both domains, however the profile nodes in overhang zone belong exclusively to the conjugate morphodynamic domain. After avalanche (slide) of the submerged zone, due to over steepening of bank-toe, the profile nodes as well as FE-nodes in this zone are projected on a slope with angle of ϕ^c . This yields in lateral displacement of the undercutting front. The rise of water stage in the river above the lower edge of the overhang results in tensile failure of the submerged overhang, which is modeled by eliminating the nodes defining undercutting front and overhang outer edge. New nodes in profile domain are generated in place of these nodes along the new water stage.

By the failure of the overhang all of the exclusive nodes in profile domain are omitted and both

domains turns to be identical (state 3 in Fig.2). By further advancement of erosion new undercutting front and overhang (outer) edge nodes are generated.

By cantilever failure of the overhang, a positive slope $\phi'' \approx 90^\circ$ is allowed here, which is determined by calibration. More studies is required to define this angle analytically by considering different parameters such as pore pressure distribution in the overhang, water stage in the river, effect of the vegetation root reinforcement and shape of the overhang block.

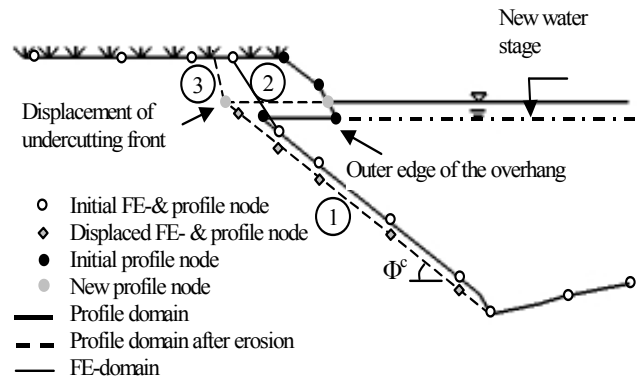


Figure 2. Conjugate numerical domains for simulation of bank erosion with complex geometry.

As it is observed in Fig. (2) , if the undercutting front does not coincides with a FE node, a new exclusive node is generated within morphological domain with no counterpart in FE domain. Depending on the element size, this may introduce a minor deviation between the flow field in FE domain and the real flow field that would have existed in the morphodynamic domain. However, this is close to the lateral boundary and near water level, which should introduce minimum error in the flow field near bank zone.

4 VERIFICATION DATA

To study riverbank erosion in non-cohesive (sandy) soils, an intensive field measurement was conducted along a river bend of a small shallow river, Hardebek-Brokenlander Au in North of Germany, by the authors (Nasermoaddeli and Pasche,2008). The river discharges into the upper reach of the river Stoer near Neumuenster and had been restored to a natural form in 2002. The bed and bank of river is composed of mainly fine sand ($d_{50}=0.2$ mm) and the bank top is covered with vegetation during the whole year.

Bank profile was measured using 3D terrestrial laser scanner between October 2006 and March 2008, intermittently. Bathymetry was measured using RTK-GPS. Three cross sections along the

river bend (entrance to the bend, upstream of the bend apex and at bend apex) were selected for verifying the new developed morphodynamic model. Flow and water level was monitored once from January to April 2007 and another time during the same period in 2008. The largest flood event occurred in January 2007 (Fig. 3), which forms the current simulation period.

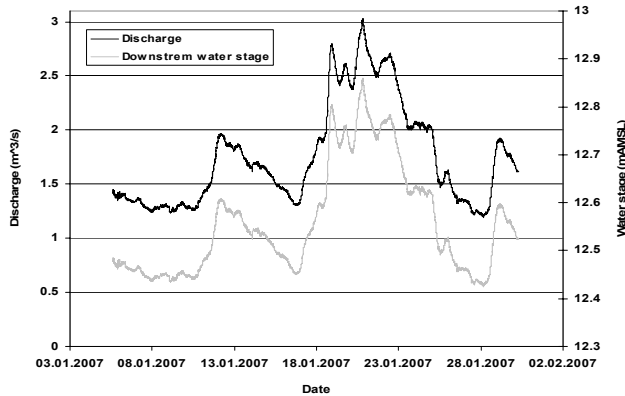


Figure 3. Discharge and water level hydrograph used for morphodynamic simulation.

5 SIMULATION RESULTS

During the simulation period the discharge varied from 1.19 to 3.03 m³/s and sediment concentration discharging to the river reach varied from 70 to 397 mg/l. The unsteady morphodynamic simulation comprised 194 time steps with a variable duration (6 minutes to 20 hours).

The result of simulation of bank retreat for the period of January 5 to March 30, 2007 using the new developed morphodynamic model has been presented in Fig. (4 and 5). Since almost no bank retreat was measured at entrance section to the bend, the result of simulations for this section has not been presented in these figures.

To account for cementation and consolidation, an increased critical (saturated) angle of repose $\phi^c=60^\circ$ and unsaturated critical angle of repose of $\phi^u=84^\circ$ for overhang zone have been applied. The lump method of distribution of waste bank material has been applied, since the other mentioned method was accompanied with instability in few time steps. A quadratic function was applied for simulation of negative pore pressure distribution over water table by considering equilibrium with water stage in the river.

As it is observed from Fig. (4), the model has been able to predict bank profile precisely at the section upstream of the bend apex, however, the bank retreat of bank top at bend apex has been over-predicted (68% error). In both cases, satisfactory results could not be attained in bank-toe zone. At the first section bed elevation has been

under-predicted, while at the second section it has been over-predicted. That can be correlated to four major factors. First, the applied hydrodynamic model does not include dispersion terms to consider the effect of secondary currents in increase of bed shear stress towards the bend apex. Nevertheless, the current available dispersion models are based on simplified assumptions, which hold only on the center line of a circular channel (Yalin, 1992) and over-predict the shear stress at outer bend (Hafner, 2008). Second, the total sediment transport model applied here is a simple model that does not account for the non-equilibrium bed load transport across river bend and the effect of secondary currents are not either considered in bed load transport. Third, the applied bed evolution model does not account for bed load transport effect (Exner equation) but total load. Fourth, the lump distribution of the failed bank materials may lead to erroneous distribution of material at bank-toe in river bend.

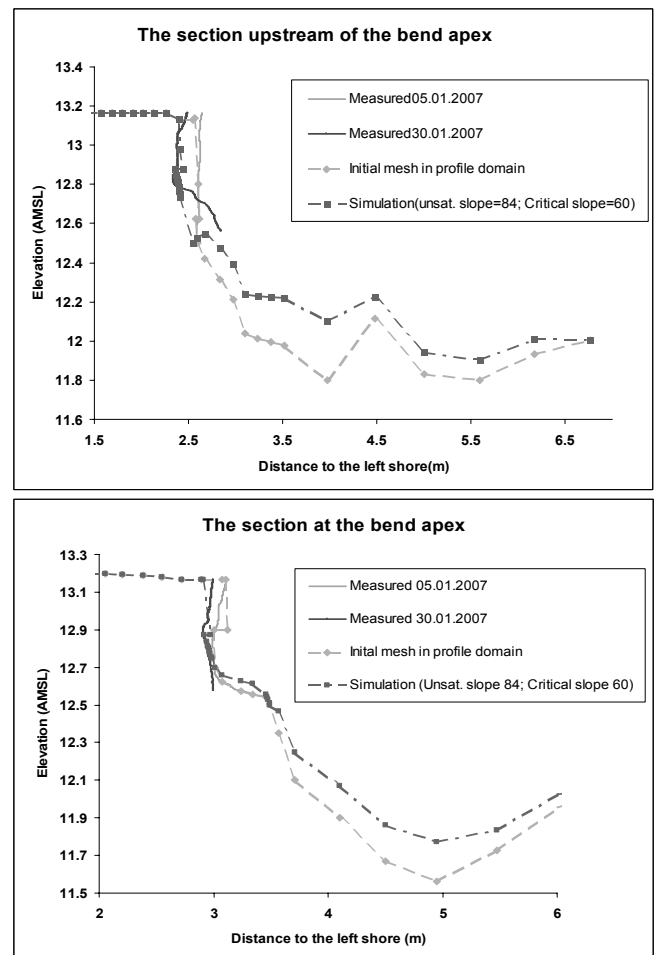


Figure 4. Bank profile before and after 25 simulated days compared with measurements.

To compare the simulation results with current practice of non-cohesive bank erosion modeling, a simulation using one critical angle of repose ($\phi^c=60^\circ$), here on called 1-slope, and a simulation without considering negative pore pressure function with two slopes, namely, $\phi^c=60^\circ$ and ϕ^u

=84°, here on called 2- slopes, were achieved. The result of this comparison is presented in Fig.(5).

As it is observed from this figure, the current approach has extremely enhanced the capability of simulation of the riverbank retreat in both sections. The comparison of the amount of the over-predication of the bank retreat using the mentioned three methods in respect to the actual bank retreat has been presented in table(1).

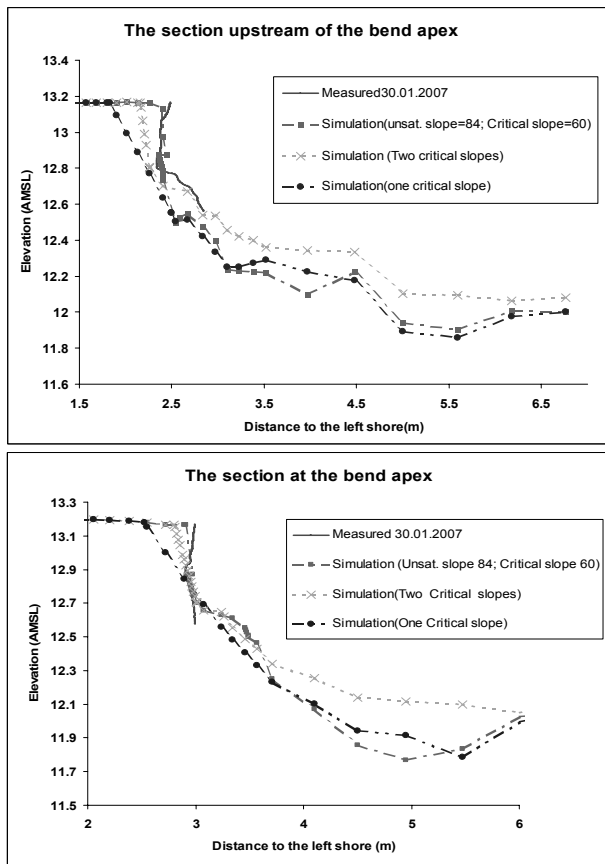


Figure 5 . Comparison of the application of the new model and earlier methods of simulation of bank erosion.

As it is observed from this table, the new morphological model were up to 6 time more accurate than the traditional 1-slope method. Although the 2-slope method improves the simulation result, however neglecting effect of the negative pore pressure deteriorates the simulation accuracy up to two times.

Table 1. Comparison of the amount of over-predication (%) of the bank retreat using three described methods

Over-predication(%)	Current model	1-slope	2-slopes
Upstream of apex	≈0*	280	100
At apex	68	392	150

* Disregarding a small vegetated zone hanged from the top of the bank by means of vegetation roots.

6 CONCLUSION

Based on the high resolution field measurements, a novel approach has been developed to model

bank erosion process in non-cohesive (sandy) soils that improves appreciably the accuracy of bank retreat modeling in such soils. Undercutting of non-cohesive riverbanks due to the bank-toe erosion and cantilever failure (shear and tensile types) have been considered in this concept. Furthermore, the effect of negative pore water pressure was approximated using an analytical function. Inclusion of such a function gained an improvement of more than double fold in simulation of bank retreat. By comparing the traditional method of non-cohesive bank erosion simulation (1-slope models) with the new developed method, up to nearly 6 fold accuracy has been attained in simulation of bank retreat at two cross sections along a river bend during one month flooding period.

Further investigation is required to improve the stability analysis of the overhang failure in sandy soils (both shear and tensile types). In the current work, undercutting due to sapping failure was not considered. A comprehensive study of the effect of pore pressure dynamic in sapping failure of non-cohesive riverbanks is recommended. The mechanism of distribution of wasted mass on bank-toe is an issue which needs more investigation and plays an important role in long-term simulation. Finally, the effectiveness of the proposed model should be further examined in long-term simulation.

ACKNOWLEDGEMENT

The first author would like to appreciate the German Federal Ministry of Education for granting IPSWaT scholarship.

REFERENCES

- ASCE Task Committee, 1998a. River width adjustment. I : Processes and Mechanisms. J. Hydr. Eng. ASCE. 124(9), 881-902.
- ASCE Task Committee, 1998b. River width adjustment. II : Modeling. J. Hydr. Eng. ASCE. 124(9), 903-917.
- Cancienne, RM., Fox, GA. and Simon, A., 2008. Influence of seepage undercutting on the stability of root-reinforced streambanks. Earth Surf. Process. Landforms. 33, 1769–1786.
- Carson, MA. and Kirkby, MJ., 1972. Hillslope form and process. University press, Cambridge.
- Casagli, N., Curini, A., Cargini, A., Rinaldi, M., Simon, A., 1997. Effects of pore water pressure on the stability of stream banks: preliminary results from the Sieve river, Italy. In: Wang, S.S.Y., Langendoen, E.J., Shields, F.D.Jr. (Eds.), Management of landscapes distributed by channel incision. 243-248.
- Casagli, N., Rinaldi, M., Cargini, A., Curini, A., 1999. Pore water pressure and stream bank stability: results from a monitoring site on the sieve river, Italy. Earth Surf.

- Process. Landforms, John Wiley and Sons, 24, 1095-114.
- Chen, D. and Duan, J.G., 2006. Modeling width adjustment in meandering channels. *Journal of Hydrology*. 321, 59-76.
- Curini, A., 1998. Analisi dei processi di sponda nei corsi d'acqua, Università degli Studi di Firenze, Dipartimento di Scienze della Terra, 147, unpublished thesis.
- Dapporto, S. Rinaldi, M. Casagli, N., 2001. Failure mechanisms and pore water pressure conditions: Analysis of a riverbank along the Arno river (Central Italy). *Engineering Geology*, Elsevier. 61: 221-242.
- Dapporto, S. Rinaldi, M. Casagli, N. Vannocci, P., 2003. Mechanics of riverbank failure along the Arno river, Central Italy. *Earth Surf. Process. Landforms*, John Wiley and Sons, 28(12), 1303-1323.
- Darby, S.E., Thorne, C.R., 1996. Numerical simulation of widening and bed deformation of straight sand-bed rivers. I: model development. *J. Hydr. Engrg. ASCE*. 122(4), 184-193.
- Darby, S.E., Gessler, D., Thorne, C.R., 2000. Technical communications-Computer program for stability analysis of steep, cohesive riverbanks. *Earth Surf. Process. Landforms*, 25, 175-190.
- Darby, S.E., Rinaldi, M. and Dapporto, S., 2007. Coupled simulations of fluvial erosion and mass wasting for cohesive river banks. *J. Geophysical Res.* 12(F03022), 1-15.
- Duan, J.G., Wang, S.S.Y., Jia, Y., 2001. The application of enhanced CCHE2D model to study alluvial channel migration processes. *J. Hydr. Res.* 39(5), 1-12.
- Forkel, C., 1995. Die Grobstruktursimulation turbulente Strömungs- und Stoffausbereitungsprozesse in Komplexen Geometrien. Bericht Nr. 24, Institut für Wasserbau und Wasserwirtschaft RWTH Aachen, Aachen.
- Fox, G.A., Wilson, G.V., Simon, A. and Langendoen E.J., Akay, O. and Fuchs, J.W., 2007. Measuring streambank erosion due to ground water seepage: correlation to bank pore water pressure, precipitation and stream stage. *Earth Surf. Process. Landforms*, 32, 1558-1573.
- Fredlund, D.G., Rahardjo, H., 1993. Soil mechanics for unsaturated soils. John Wiley and Sons. 1993. Pp.517.
- Hafner, T., 2008. Uferrückbau und eigendynamische Gewässerentwicklung: Aspekte der Modellierung und Abschätzungsmöglichkeiten in der Praxis. berichte des Lehrstuhls und der Versuchsanstalt für Wasserbau und Wasserwirtschaft der TU München, Nr.117.
- Hagerty, D.J., 1991. Piping/sapping erosion. I : Basic considerations. *J. Hydr. Engrg. ASCE*. 117(8), 991-1008.
- Hasegawa, K., 1981. Bank erosion discharge based on a non-equilibrium theory. *Proc. JSCE*, Tokyo, 316, 37-50 (in Japanese).
- Jang, C.L. and Shimizu, Y., 2005. Numerical simulation of relatively wide, shallow channels with erodible banks. *J. Hydr. Eng. ASCE*. 131(7), 565-575.
- King, I.P., 2005. A finite element model for flow and cohesive/ sand transport RMA10s.: User guide, Version 3.3. Resource Modelling Associates, Sydney, NSW, Australia. Pp.87.
- Kovacs, A., Parker, G., 1994. A new vectorial bed load formulation and its application to the time evolution of straight river channels, *J. Fluid Mech.*, 267, 153-183.
- Langendoen E.J., Simon, A., 2008. Modeling the Evolution of Incised Streams. II: Streambank Erosion. *J. Hydr. Engrg. ASCE*. 134(7), 905-915
- Lawler, D.M., Couperthwaite, J. Bull, L., Haris, M.N., 1997. Bank erosion events and processes in the Upper Seven Basin. *Hydrology and Earth systems Science*. 1, 523-534.
- Mosselman, E., 1992. Mathematical modeling of morphological processes in rivers with erodible cohesive banks. PhD thesis, Delft, the Netherlands.
- Nagata, T. Hosoda, T. Muramoto, Y., 2000. Numerical analysis of river channel processes with bank erosion. *J. Hydr. Eng. ASCE*. 126(4), 243-252.
- Nasermoaddeli, M.H., Pasche E., 2008. Application of terrestrial 3D laser scanner in quantification of the riverbank erosion and deposition. In: *Proceedings of Riverflow 2008*, Cesme-Ismir, Turkey, Sep. 3-5, Vol. (3), 2407-2416.
- Osman, A.M., Thorne, C.R., 1998. River bank stability analysis. I: Theory. *J. Hydr. Engrg. ASCE*. 114(2), 134-150.
- Phillips, B.C., Sutherland, A.J., 1989. Spatial and lag effects in bed load sediment transport. *Journal of Hydraulic Research*, 27, 115-122.
- Rinaldi, M. Casagli, N., Dapporto, S., Gargini, A., 2004. Monitoring and modeling of pore water pressure changes and riverbank stability during flow events. *Earth Surf. Process. Landforms*, John Wiley and Sons, 29(2), 237-254.
- Rinaldi, M., Mengoni, B., Luppi, L., Darby, S.E., 2008. Numerical Simulation of hydrodynamics and bank erosion in a river bend. *Water resources research*, 44(W09428). 1-17; DOI:10.1029/2008WR007008.
- Rodi, W., 1993. Turbulence models and their application in hydraulics: A state-of-art review. IAHR. A.A. Balkema, Rotterdam, Netherland. Pp.104.
- Shimizu, Y., Hirano, N., Wanatabe, Y., 1996. Numerical calculation of bank erosion and free meandering. *Annu. J. Hydr. Engrg. JSCE*, 40, 921-926 (in Japanese).
- Schmautz, M., 2003. Eigendynamische Aufweitung in einer geraden Gewässerstrecke- Entwicklung und Untersuchungen an einem numerischen Model. *Berichte des Lehrstuhls und der Versuchsanstalt für Wasserbau und Wasserwirtschaft der TU München*, Nr.96.
- Simon, A., Curini, A., Darby, S.E., Langendoen, E.J., 2000. Bank and near-bank processes in incised channel. *Geomorphology*, 35(3), 193-217.
- Simon, A., Collison, A.J.C. Layzell, A., 2003. Incorporating bank-toe erosion by hydraulic shear into ARS bank stability model: Missouri River, Eastern Montana. *Proc. of World Water and Environmental Resources Congress*, June 23-26, 2003, Philadelphia, PA. USA. (published on digital media, CD).
- Thorne, C.R. And Tovey, N.K., 1981. Stability of composite river banks. *Earth Surf. Process. Landforms*, 6, 469-484.
- Thorne, C.R., 1982. Processes and mechanisms of river bank erosion. In: *Gravel-Bed Rivers*, R.D. Hey, J.C. Bathurst and C.R. Thorne, (Eds), John Wiley and Sons, Chichester, England. 227-272.
- Ullrich, C.R., Hagerty, D.J., Holmberg, R.W., 1986. Surficial failures of alluvial stream banks. *Can. Geotech. J.*, 23(3), 304-316.
- van Rijn, L.C., 1984a. Sediment transport. I: Bed load transport. *J. Hydr. Engrg. ASCE*. 110(10): 1431-1456.
- van Rijn, L.C., 1984b. Sediment transport. II: Suspended load transport. *J. Hydr. Engrg. ASCE*. 110(11): 1613-1641.
- Wilson, G.V., Periketi, R.K., Fox, G.A., Dabney, S.M., Shields, F.D., and Cullum, R.F., 2007. Soil properties controlling seepage erosion contributions to streambank failure. *Earth Surf. Process. Landforms*. 32, 447-459.
- Yalin, M.S., 1992. River mechanics. Pergman Press Ltd, Oxford, England. Pp.220.